

## Bragg grating rogue wave



Antonio Degasperis<sup>a</sup>, Stefan Wabnitz<sup>b,\*</sup>, Alejandro B. Aceves<sup>c</sup>

<sup>a</sup> Dipartimento di Fisica, "Sapienza" Università di Roma, P.le A. Moro 2, 00185 Roma, Italy

<sup>b</sup> Dipartimento di Ingegneria dell'Informazione, Università degli Studi di Brescia and INO-CNR, via Branze 38, 25123 Brescia, Italy

<sup>c</sup> Southern Methodist University, Dallas, USA

### ARTICLE INFO

#### Article history:

Received 21 January 2015

Accepted 23 January 2015

Available online 28 January 2015

Communicated by V.M. Agranovich

#### Keywords:

Nonlinear waves

Nonlinear optics

Optical fibers

Periodic media

Water waves

### ABSTRACT

We derive the rogue wave solution of the classical massive Thirring model, that describes nonlinear optical pulse propagation in Bragg gratings. Combining electromagnetically induced transparency with Bragg scattering four-wave mixing may lead to extreme waves at extremely low powers.

© 2015 Elsevier B.V. All rights reserved.

## 1. Introduction

Extreme wave phenomenon appears in a variety of scientific and social contexts, ranging from hydrodynamics and oceanography to geophysics, plasma physics, Bose–Einstein condensation (BEC), financial markets and nonlinear optics [1–5]. Historically, the first reported manifestation of extreme or rogue waves is the sudden appearance in the open sea of an isolated giant wave, with height and steepness much larger than the average values of ocean waves. A universal model for describing the dynamics of rogue wave generation in deep water with a flat bottom is the one-dimensional nonlinear Schrödinger (NLS) equation in the self-focusing regime. The mechanism leading to the appearance of NLS rogue waves requires nonlinear interaction and modulation instability (MI) of the continuous wave (CW) background [6]. Indeed, the nonlinear development of MI may be described by families of exact solutions such as the Akhmediev breathers [7], which are recognized as a paradigm for rogue wave shaping. A special member of this solution family is the famous Peregrine soliton [8], which describes a wave that appears from nowhere and disappears without a trace. Extreme waves that may be well represented by the Peregrine soliton have recently been experimentally observed in optical fibers [9], in water-wave tanks [10] and in plasmas [11].

Moving beyond the one-dimensional NLS model, it is important to consider extreme wave phenomenon in either multidimen-

sional or multicomponent nonlinear propagation. Vector systems are characterized by the possibility of observing a coupling of energy among their different degrees of freedom, which substantially enriches the complexity of their rogue-wave families. Recent studies have unveiled the existence of extreme wave solutions in the vector NLS equation or Manakov system [12–15], the three-wave resonant interaction equations [16], the coupled Hirota equations [17] and the long-wave–short-wave resonance [18].

In this Letter, we present the rogue wave solution of the classical massive Thirring model (MTM) [19], a two-component nonlinear wave evolution model that is completely integrable by means of the inverse scattering transform method [20–22]. The classical MTM is a particular case of the coupled mode equations (CMEs) that describe pulse propagation in periodic or Bragg nonlinear optical media [23–27]. Furthermore, the CMEs also appear in other physical settings. In particular and relevant to rogue waves, they describe ocean waves in deep water for a periodic bottom [28]. As such, the search for novel solution forms of these equations including rogue waves, provides understanding of nonlinear phenomenon and leads to applications beyond optical systems. In this respect, benefiting from the result [25,29] that many MTM solutions (including single and multi-solitons and cnoidal-waves) may be mapped into solutions of the CMEs, provides a tool used in several works including ocean waves [30], BEC [31] and metamaterials [32].

After discussing the analytical rogue wave solution in Section 2, in Section 3 we numerically confirm its stability, and show that it may also be applied to describe the generation of extreme events

\* Corresponding author.

E-mail address: stefan.wabnitz@unibs.it (S. Wabnitz).

in the more general context of the CMEs. Finally, in Section 4 we discuss the physical implementation of MTM rogue waves by using coherent effects in resonant nonlinear media, such as electromagnetically induced transparency (EIT), which may lead to the giant enhancement of cross-phase modulation (XPM) with the simultaneous suppression of self-phase modulation (SPM).

## 2. Analytical solution

Let us express the MTM equations for the forward and backward waves with envelopes  $U$  and  $V$ , respectively, as

$$\begin{aligned} U_\xi &= -i\nu V - \frac{i}{\nu}|V|^2 U \\ V_\eta &= -i\nu U - \frac{i}{\nu}|U|^2 V. \end{aligned} \quad (1)$$

Here the light-cone coordinates  $\xi, \eta$  are related to the space coordinate  $z$  and time variable  $t$  by the relations  $\partial_\xi = \partial_t + c\partial_z$  and  $\partial_\eta = \partial_t - c\partial_z$ , where  $c > 0$  is the linear group velocity. Even though the arbitrary real parameter  $\nu$  can be rescaled to unity, we find it convenient to keep it for dimensional reasons.

The rogue waves travel over the following CW background

$$U_0 = ae^{i\phi}, \quad V_0 = -be^{i\phi} \quad (2)$$

where, with no loss of generality, the constant amplitudes  $a$  and  $b$  are real, and the common phase  $\phi(\xi, \eta)$  is

$$\phi = \alpha\xi + \beta\eta, \quad \alpha = b\left(\frac{\nu}{a} - \frac{b}{\nu}\right), \quad \beta = a\left(\frac{\nu}{b} - \frac{a}{\nu}\right). \quad (3)$$

Up to this point we consider the two amplitudes  $a, b$  as free background parameters. It can be proved that rogue wave solutions of Eqs. (1) exist if and only if the two amplitudes  $a, b$  satisfy the inequality

$$0 < ab < \nu^2. \quad (4)$$

By applying the Darboux method to the MTM [33], one obtains the following rogue wave solution

$$\begin{aligned} U &= ae^{i\phi} \frac{\mu^*}{\mu} \left(1 - 4i \frac{q_1^* q_2}{\mu^*}\right), \\ V &= -be^{i\phi} \frac{\mu}{\mu^*} \left(1 - 4i \frac{q_1^* q_2}{\mu}\right) \end{aligned} \quad (5)$$

with the following definitions

$$\begin{aligned} q_1 &= \theta_1(1 + iq) + q\theta_2, \quad q_2 = \theta_2(1 - iq) + q\theta_1, \\ q &= \frac{a}{\chi^*} \eta + b\chi^* \xi \end{aligned} \quad (6)$$

and

$$\begin{aligned} \mu &= |q_1|^2 + |q_2|^2 + (i/p)(|q_1|^2 - |q_2|^2), \\ p &= \sqrt{\frac{\nu^2}{ab} - 1} > 0. \end{aligned} \quad (7)$$

In the expression (5), which is the analog of the Peregrine solution of the focusing NLS equation, the free parameters are the two real background parameters  $a, b$ , which are however constrained by the condition (4), and the two complex parameters  $\theta_1, \theta_2$ , while the parameter  $\chi$  is given by the expression

$$\chi = \frac{b}{\nu}(1 + ip) = \frac{\nu}{a(1 - ip)}. \quad (8)$$

Expression (5) of the rogue wave solution may be simplified by fixing the reference frame of the space–time coordinates. The general solution (5) may then be obtained by applying to this particular solution a Lorentz transformation.

According to the last remark above, we now provide the rogue wave solution in terms of the space  $z = c(\xi - \eta)$  and time  $t = (\xi + \eta)$  coordinates directly. By rewriting the CW phase (3) in these coordinates, one obtains

$$\begin{aligned} \phi &= kz - \omega t, \quad k = \frac{\nu}{2c} \left(1 - \frac{ab}{\nu^2}\right) \left(\frac{b}{a} - \frac{a}{b}\right), \\ \omega &= -\frac{\nu}{2} \left(1 - \frac{ab}{\nu^2}\right) \left(\frac{a}{b} + \frac{b}{a}\right), \end{aligned} \quad (9)$$

where  $k$  is the wave number of the background CW. Setting  $a = b$  means choosing the special frame of reference such that  $k = 0$ . Note that the other possibility  $a = -b$  does not satisfy the condition that  $p$  is real (see (7)). From a physical standpoint, the CW background solution with  $a = b$  corresponds to a nonlinear wave whose frequency  $\omega = -\nu(1 - a^2/\nu^2)$  enters deeper inside the (linear) forbidden band-gap  $\omega^2 < \nu^2$  as its intensity grows larger. A linear stability analysis of the CW background solution (2) shows that it is modulationally unstable for perturbations with a wavenumber  $k^2 < 4a^2/c^2$  (for details, see [34]). Note that modulation instability gain extends all the way to arbitrarily long-scale perturbations (albeit with a vanishing gain), a condition which has been referred to as “baseband instability”, and that is closely linked with the existence condition of rogue waves in different nonlinear wave systems (e.g., the Manakov system, see Ref. [15]). It is also interesting to point out that, outside the range of existence of the rogue wave solution (5), that is for  $a^2 > \nu^2$ , the background is unstable with respect to CW perturbation with a finite (nonzero) gain (see Ref. [34]).

By using translation invariance to eliminate the parameters  $\theta_1, \theta_2$ , one finally ends up with the following expression of the MTM rogue wave solution

$$\begin{aligned} U &= ae^{-i\omega t} \frac{\mu^*}{\mu} \left[1 - \frac{4}{\mu^*} q^*(q + i)\right], \\ V &= -ae^{-i\omega t} \frac{\mu}{\mu^*} \left[1 - \frac{4}{\mu} q^*(q + i)\right] \end{aligned} \quad (10)$$

where

$$\begin{aligned} \omega &= -\nu \left(1 - \frac{a^2}{\nu^2}\right), \quad q = -\frac{a^2}{\nu c} [ip(z - z_0) - c(t - t_0)], \\ p &= \sqrt{\frac{\nu^2}{a^2} - 1}, \quad \mu = 2|q|^2 + (1 + 2\text{Im} q) \left(1 - \frac{i}{p}\right), \end{aligned} \quad (11)$$

where  $z_0$  and  $t_0$  are arbitrary space and time shifts, respectively. Note that a further simplification may come from rescaling  $z, t, U, V$  by using the length scale factor  $S = -\nu c/a^2$ .

In Fig. 1 we show the dependence on space and time of the intensities  $|U|^2$  and  $|V|^2$  of the forward and backward components of the rogue wave (10). Here we have set  $\nu = -1, c = 1, a = 0.9, t_0 = 2$  and  $z_0 = 3.5$ . As can be seen, the initial spatial modulation at  $t = 0$  evolves into an isolated peak with a maximum intensity of about *nine times* larger than the CW background intensity. The corresponding contour plot of these intensities is shown in Fig. 2.

## 3. Numerical results

In order to verify the spatio-temporal stability of the rogue wave solution (10) over a finite spatial domain, we numerically solved Eqs. (1) with  $\nu = -1, c = 1$ , and using the initial (i.e., at  $t = 0$ ) and boundary (i.e., at  $z = 0$  and  $z = L$ ) conditions given by

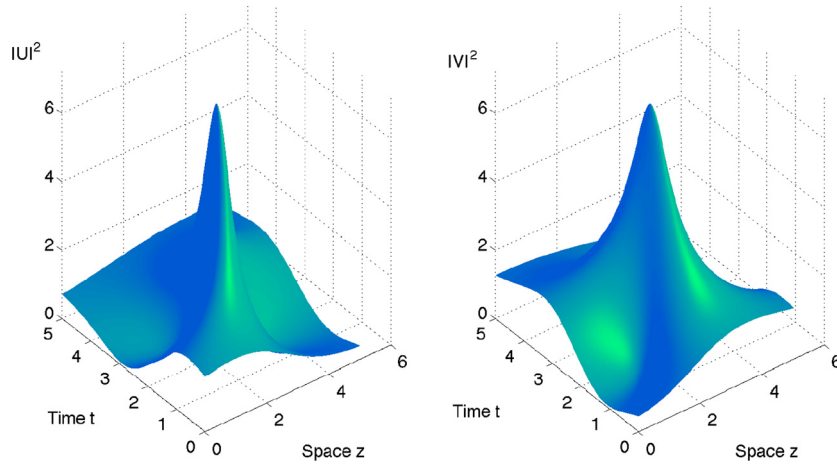


Fig. 1. Evolution in time and space of the intensities in the forward and backward components of the rogue wave solution (10).

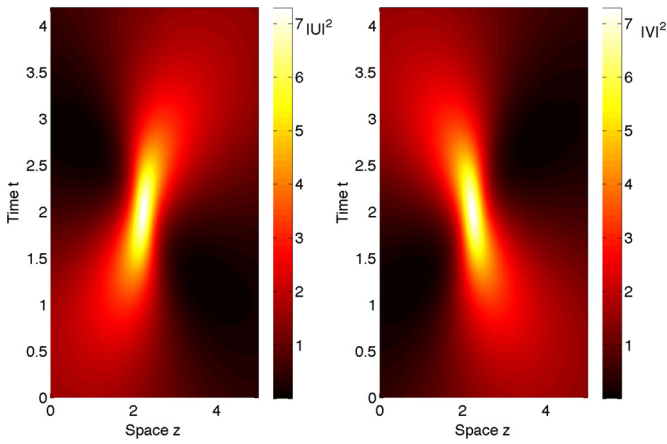


Fig. 2. Contour plot of the intensities of the forward and backward waves as in Fig. 1.

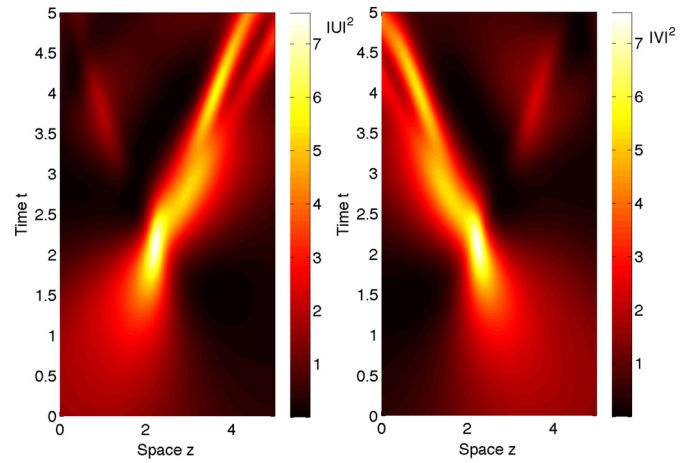


Fig. 4. Numerical solution of CMEs with  $\sigma = 0.3$  and initial and boundary conditions as given by the analytical solution of Fig. 1.

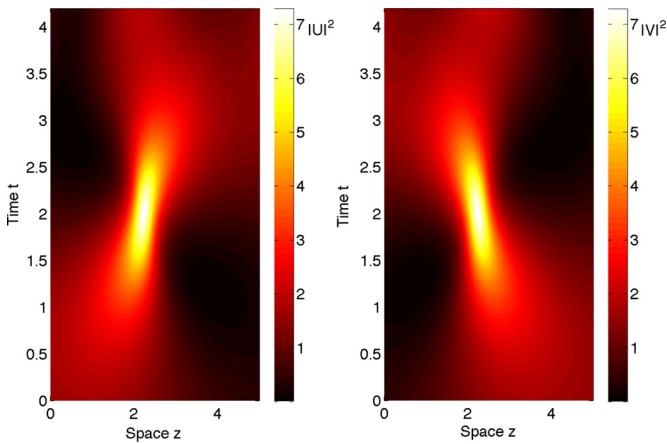


Fig. 3. Numerical solution corresponding to the analytical solution in Fig. 1.

the exact expression (10), with the same solution parameters as in Figs. 1–2, and with  $L = 5 \simeq 4S$ .

Fig. 3 displays the numerically computed intensities of the forward and backward waves: as it can be seen, there is an excellent agreement with the analytical solution. This confirms the stability and observability of the rogue wave solution (10), in spite of in the presence of the competing background MI.

At this point it is quite natural, and interesting, to numerically check whether the initial conditions of the rogue wave so-

lution (10) may induce also the generation of a rogue wave as modeled by the CMEs for pulse propagation in nonlinear Bragg gratings [25] or ocean waves with periodic bottom [28]. Indeed, the CMEs

$$\begin{aligned} U_\xi &= -i\nu V - \frac{i}{\nu} (|V|^2 + \sigma|U|^2)U, \\ V_\eta &= -i\nu U - \frac{i}{\nu} (|U|^2 + \sigma|V|^2)V \end{aligned} \quad (12)$$

differ from the MTM Eqs. (1) by an additional SPM term, its relative strength being expressed by the coefficient  $\sigma$ . We have numerically solved Eqs. (12) with initial and boundary conditions as given by expression (10). As shown by Fig. 4 and Fig. 5, quite surprisingly even in the case of a comparatively large SPM contribution, one still observes the generation of an extreme peak with nearly the same intensity and time width as in the MTM case. However now the peak no longer disappears, but it leaves behind traces in the form of dispersive waves, owing to the non-integrability nature of the CMEs. In Fig. 4 we set  $\sigma = 0.3$ , while qualitatively very similar results are also obtained for larger values of  $\sigma$  (e.g., for  $\sigma = 0.5$ , which corresponds to the case of nonlinear fiber gratings).

On the other hand, in Fig. 5 we show the case with  $\sigma = -0.5$ , that is relevant to water wave propagation in oceans with a periodic bottom [28]. Interestingly, in the hydrodynamic case the formation of a first rogue peak where both components have nearly the same amplitude as in the MTM case Fig. 3, is followed by wave

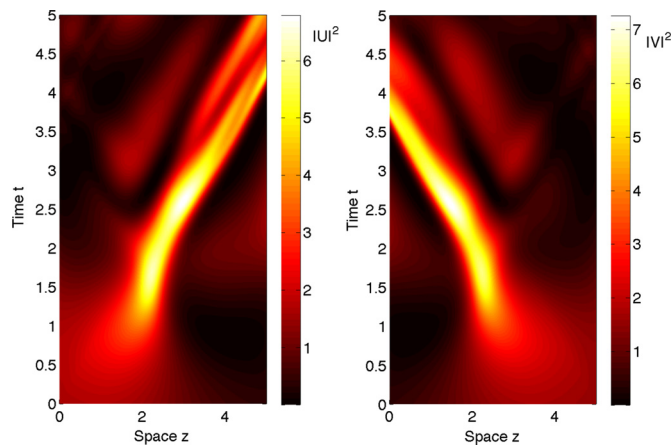


Fig. 5. As in Fig. 4, with  $\sigma = -0.5$ .

breaking into secondary, and yet intense peaks in each of the two generated pulses that travel in opposite directions.

#### 4. Discussion and conclusions

For the strict applicability of the analytical MTM rogue wave solution (10) of Section 2, it is necessary that SPM can be neglected with respect to XPM. This situation occurs whenever the forward and backward wave envelopes have different carrier frequencies, say,  $\omega_U$  and  $\omega_V$ , and their frequency difference  $\Delta\omega = \omega_U - \omega_V$  is close to a resonant frequency of the nonlinear medium [35]. Whenever the forward and backward waves are coherently coupled in a four-level atomic system by a CW pump field, a giant enhancement of the strength of XPM is also possible via the EIT effect [36,37], with no competing SPM. In addition, EIT brings the important benefit of zero linear absorption losses, and it is only limited by the residual two-photon absorption, which can be neglected for relatively short interaction distances.

For maximizing the interaction length of the counter-propagating waves, diffraction effects can be suppressed by using an atomic vapor cell containing an hollow-core photonic band gap fiber (PBGF). A scheme of Bragg soliton generation in a coherent medium exhibiting EIT has been previously discussed, however counter-propagating pulses at the same probe frequency were considered [38]. A dynamic refractive index grating for coupling forward and backward signal waves at different frequencies may be induced by the standing wave generated from the beating of two counter-propagating pump waves, with a frequency difference equal to  $\Delta\omega$ . This process is known as Bragg scattering four-wave mixing (BS-FWM) [39], and it enables noise-free frequency translation. Indeed, BS-FWM in the co-propagation geometry and at microwatt pump power levels has been recently demonstrated in Rubidium vapor, confined to a few centimeters long PBGF [40].

Note that the solution (10) may also apply to describe extreme wave emergence in the co-propagation of two signals at different carrier frequencies [41], by simply interchanging the role of time and space variables in Eqs. (1). In this case, a dynamic grating may be induced by the beating of two pump waves in the orthogonal polarization [42].

In short summary, we obtained the rogue wave solution of the classical MTM, which extends the Peregrine soliton solution of the NLS equation to the case of wave propagation in a periodic

nonlinear medium. An implementation is proposed using coherent resonant wave mixing: we envisage that Bragg solitons and rogue waves may ultimately be observed at sub-milliwatt pumping levels by using chip-scale waveguides that are evanescently coupled to atomic vapors [43].

#### Acknowledgements

The present research was supported by Fondazione Cariplo, grant No. 2011-0395, and the Italian Ministry of Education, Research and Universities (MIUR) (grant contract 2012BFNWZ2).

#### References

- [1] D.R. Solli, C. Ropers, P. Koonath, B. Jalali, *Nature* 450 (2007) 1054.
- [2] K. Dysthe, H.E. Krogstad, P. Muller, *Annu. Rev. Fluid Mech.* 40 (2008) 287.
- [3] N. Akhmediev, E. Pelinovsky, *Eur. Phys. J. Spec. Top.* 185 (2010) 1.
- [4] M. Onorato, S. Residori, U. Bortolozzo, A. Montina, F.T. Arecchi, *Phys. Rep.* 528 (2013) 47.
- [5] J.M. Dudley, F. Dias, M. Erkintalo, G. Genty, *Nat. Photonics* 8 (2014) 755.
- [6] T.B. Benjamin, J.E. Feir, *J. Fluid Mech.* 27 (1967) 417.
- [7] N. Akhmediev, V.I. Korneev, *Theor. Math. Phys. (USSR)* 69 (2) (1986) 189; translation from Russian, *Theor. Math. Phys. (USSR)* 69 (2) (1986) 1089.
- [8] D.H. Peregrine, *J. Aust. Math. Soc. Ser. B, Appl. Math* 25 (1983) 16.
- [9] B. Kibler, J. Fatome, C. Finot, G. Millot, F. Dias, G. Genty, N. Akhmediev, J.M. Dudley, *Nat. Phys.* 6 (2010) 790.
- [10] A. Chabchoub, N.P. Hoffmann, N. Akhmediev, *Phys. Rev. Lett.* 106 (2011) 204502.
- [11] H. Bailung, S.K. Sharma, Y. Nakamura, *Phys. Rev. Lett.* 107 (2011) 255005.
- [12] F. Baronio, A. Degasperis, M. Conforti, S. Wabnitz, *Phys. Rev. Lett.* 109 (2012) 044102.
- [13] L.C. Zhao, J. Liu, *Phys. Rev. E* 87 (2013) 013201.
- [14] B.G. Zhai, W.G. Zhang, X.L. Wang, H.Q. Zhang, *Nonlinear Anal., Real World Appl.* 14 (2013) 14.
- [15] F. Baronio, M. Conforti, A. Degasperis, S. Lombardo, M. Onorato, S. Wabnitz, *Phys. Rev. Lett.* 113 (2014) 034101.
- [16] F. Baronio, M. Conforti, A. Degasperis, S. Lombardo, *Phys. Rev. Lett.* 111 (2013) 114101.
- [17] S. Chen, L.Y. Song, *Phys. Rev. E* 87 (2013) 032910.
- [18] S. Chen, Ph. Grelu, J.M. Soto-Crespo, *Phys. Rev. E* 89 (2014), 011201(R).
- [19] W. Thirring, *Ann. Phys.* 3 (1959) 91.
- [20] A.V. Mikhailov, *JETP Lett.* 23 (1976) 320.
- [21] E.A. Kuznetsov, A.V. Mikhailov, *Teor. Mat. Fiz.* 30 (1977) 193.
- [22] D.J. Kaup, A.C. Newell, *Lett. Nuovo Cimento* 20 (1977) 325.
- [23] H.G. Winful, G.D. Cooperman, *Appl. Phys. Lett.* 40 (1982) 298.
- [24] D.N. Christodoulides, R.I. Joseph, *Phys. Rev. Lett.* 62 (1989) 1746.
- [25] A.B. Aceves, S. Wabnitz, *Phys. Lett. A* 141 (1989) 37.
- [26] B.J. Eggleton, R.E. Slusher, C.M. de Sterke, P.A. Krug, J.E. Sipe, *Phys. Rev. Lett.* 76 (1996) 1627.
- [27] B.J. Eggleton, C.M. de Sterke, R.E. Slusher, *J. Opt. Soc. Am. B* 14 (1997) 2980.
- [28] V.P. Ruban, *Phys. Rev. E* 77 (5) (2008) 055307.
- [29] A.B. Aceves, S. Wabnitz, *Nonlinear Processes in Physics, Springer Series in Nonlinear Dynamics*, 1993, p. 3.
- [30] V.P. Ruban, *Phys. Rev. E* 78 (6) (2008) 066308.
- [31] O. Zobay, S. Pötting, P. Meystre, E.M. Wright, *Phys. Rev. A* 59 (1) (1999) 643.
- [32] S. Longhi, *Waves Random Complex Media* 15 (1) (2005) 119.
- [33] A. Degasperis, arXiv:1411.7965v1, 2014.
- [34] A.B. Aceves, C. De Angelis, S. Wabnitz, *Opt. Lett.* 17 (1992) 1566.
- [35] S.A. Akhmanov, N.I. Koroteev, in: *Metody Nelineinnoi Optiki v Spektroskopii Rasseyaniya Sveta (Methods of Nonlinear Optics Light-Beating Spectroscopy)*, Nauka, Moscow, 1981, p. 139.
- [36] H. Schmidt, A. Imamoglu, *Opt. Lett.* 21 (1996) 1936.
- [37] I. Friedler, G. Kurizki, O. Cohen, M. Segev, *Opt. Lett.* 30 (2005) 3374.
- [38] W. Jiang, Q. Chen, Y. Zhang, G. Guo, *Opt. Express* 15 (2007) 7933.
- [39] C.J. McKinstrie, J.D. Harvey, S. Radic, M.G. Raymer, *Opt. Express* 13 (2005) 9131.
- [40] P.S. Donvalkar, V. Venkataraman, S. Clemmen, K. Saha, A.L. Gaeta, *Opt. Lett.* 39 (2014) 1557.
- [41] S. Wabnitz, *Opt. Lett.* 14 (1989) 1071.
- [42] G. Van Simaey, S. Coen, M. Haelterman, S. Trillo, *Phys. Rev. Lett.* 92 (2004) 223902.
- [43] I. Agha, S. Ates, M. Davanço, K. Srinivasan, *Opt. Express* 21 (2013) 21628.